Journal of Achievements in Materials and Manufacturing Engineering
VOLUME 31
ISSUE 2
December
2008

Manufacturing and damage mechanisms in metal matrix composites

E. Bayraktar [a,b,*], J. Masounave [c], R. Caplain [b], C. Bathias [b]
[a] School of Mechanical and Manufacturing Engineering,
EA 2336 Supmeca/LISMMA-Paris, France
[b] Chair of Industrial Materials Laboratory,
Conservatoire National des Arts et Métiers, Case 321, Paris, France
[c] Montréal Technical University, 2900, boul. Édouard-Montpetit,
2500, Chemin de Polytechnique, Montréal, Québec, Canada
* Corresponding author: E-mail address: bayraktar@supmeca.fr

Received 09.09.2008; published in revised form 01.12.2008

Properties

ABSTRACT

Purpose: Mechanical properties of metal matrix composites (MMCs) are essentially functions of the manufacturing processes. Surface state and roughness conditions as well as the type of matrix reinforcement and heat treatment influence the mechanical behaviour of the MMCs in service conditions. The factors such as the porosity of the matrix, volume fraction of the reinforcement and their distribution, agglomeration or sedimentation of particles and particle size, dross and porosities influence the behaviour of the MMC. The static and cyclic deformation behaviour of these two metal matrix composites has been investigated at room temperature; 2124/Al-Si-Cu fabricated by powder metallurgy and AS7G/Al-Si-Mg fabricated by foundry.
Design/methodology/approach: In cyclic deformation, surface roughness effect on the damage behaviour has been discussed. The microstructure for optical images was made by Olympus optical microscope (OM). The failed specimens are observed by using of scanning electron microscope (SEM) and also the variation of volume fraction depending on the tomography density (TD) was evaluated by means of X-rays computed tomography, CT.
Findings: AS7G composite showed considerable lower mechanical properties regarding to the 2124 composite. In the AS7G composite, the crack generally initiated at the interface (SiC/matrix) with many interface debonding between the SiC particles and the matrix. This was the principal cause of the reduced fatigue strength.
Practical implications: Applications of χ-rays CT on the composite materials is more efficient and skilful. χ-rays CT well characterise the particle size and the distribution of the reinforcements-volume fraction as 3D at the mesoscopic scale as a possible way to study this aspect.
Originality/value: Manufacturing of two new different MM-composites and damage analysis in successful usage of aerospace application.
Keywords: Metal matrix composites; Damage mechanisms; SEM

1. Introduction

The development of metal matrix composites (MMCs), is of great interest in industrial applications for lighter materials with high specific strength, stiffness and heat resistance. They form a new class of industrial materials. In MMCs, aluminium-matrix composites (AMCs) reinforced with discontinuous reinforcements are very attractive because they give the best combination of strength, ductility and toughness and they can be processed by conventional methods such as rolling, forging, extrusion and as a final process, machining. Important MMCs applications in the

ground transportation (auto and rail such as brake drums, engine pistons), thermal management, aerospace, industrial, recreational and infrastructure industries have been enabled by functional properties that include high structural efficiency, excellent wear resistance, and attractive thermal and electrical characteristics because of their higher strength and stiffness and their improved strength to weight ratio compared to non-reinforced alloys [1-11]. Challenging technical issues have been overcome, including compatibility between reinforcement and matrix, affordable primary and secondary processing techniques capable of adequately controlling reinforcement distribution, engineering design methodologies, and characterization and control of interfacial properties. MMCs are now an established materials technology. Future visions of new MMC paradigms that might underpin a new expansion have not been clearly identified and there is presently no focused effort to expand the scope of MMCs [2, 3, 7, 18-20, 27, 28].

The mechanical properties of these materials are functions of the manufacturing processes. Some factors such as surface state and roughness as well as the type of matrix, volume fraction of reinforcement, particle size and their distribution and heat treatment basically influence their mechanical behaviours particularly fatigue behaviours in service conditions. A number of studies on the mechanical characterisation of MMCs have been carried out and many different results have been reported and comprehensive information on the definition, constitution, processing, microstructures and properties of MMCs is available from other sources [1-36].

For example, in a comparative study, the surface treatment effect on the fatigue properties has been given for Al2024-T3 Alclad and Al7075-T6 alloys. This paper provided that the Fatigue properties in air are almost the same for treated and untreated samples for both alloys. There was any surface effect on the fatigue behaviour.

Therefore it is necessary to understand the damage mechanisms under different solicitations. The main objective of this study were to investigate the static and cyclic deformation behaviour at room temperature (T=24°C) for two AMCs. In the present study, hardness, tensile and fatigue tests were performed in ambient using smooth specimens in different surface conditions (as-received and polished) of the two different aluminium-matrix composites (AMCs), (2124/Al-Si-Cu and AS7G/Al-Si-Mg) and damage mechanisms are discussed. The damaged specimens are observed by using of scanning electron microscope (SEM). The variation of volume fraction depending on the tomography density (TD) was evaluated by means of X-rays computed tomography, CT, (medical scanner).

2. Manufacturing of the specimens and experimental conditions

Two series of MMCs were prepared in the laboratory of the French aeronautic company as follows:

The 1st series of samples (2124, Al-Si-Cu) with a volume fraction of 25% SiC_p reinforcement, the materials were processed by powder metallurgy technique. This processing route begins with blending matrix powder and reinforcement particles. After that, the mixture is canned and degassed to remove adsorbed or chemically bonded water or other volatile elements and then extruded with a ratio of 5:1 for further improvement density. In fact, as well shown in the literature, a wide range of thermomechanical processes have been established for particle matrix P/M, discontinuously reinforced Al (DRA), and forging, extrusion and rolling are the most widely used for the current applications in this domain [3, 18, 19, 21, 26, 27]. Additionally, to improved strength and stiffness, an attractive balance of fracture properties including ductility, toughness and fatigue are available from commercial P/M DRA materials. This is achieved through the control of V_f (which is typically limited to ~ 20%) and/or particulate size, along with the strict control of particulate distribution via initial blending and subsequent thermomechanical deformation [3, 18, 19].

The 2nd series of the samples (AS7G, Al-Si-Mg) with a volume fraction of 20% SiC_p reinforcement were fabricated by foundry. The nominal chemical compositions of these samples are given in Table 1. The particle sizes of 2124 and AS7G alloys were approximately 1and 13 µm respectively, denoted hereafter as 1 and 13 µm SiC_p/Al composites respectively. The aspect ratio of particles in composites was between 1.85 and 2.

As for the specimens of AS7G, Firstly, they were solution treated at 529°C for 12 hours, quenched in water and then tempered at 160°C for 24 hours (type T6). A complementary special heat treatment (called TS) has been carried out; they were solution treated at 549°C for 10 hours, cooled in air and then tempered at 160°C for 24 hours in order to provide good consolidation the interfacial cohesion (particle/matrix) for improving mechanical properties in severe conditions (for example at high temperature.

The flat specimens used for the tensile and fatigue tests (80x10x3) with a length of 80 mm, a width of 10 mm and the thickness of the specimens was 3 mm. They were machined from as received bars. Fig. 1 shows the geometry of the specimens used for the tensile and fatigue tests.

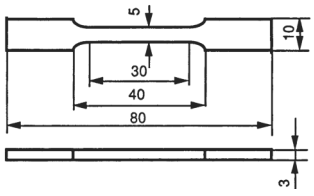

Fig. 1. Geometry of the specimens used for the static and cyclic tests

Microstructures of the AS7G and 2124 were carried out by optical microscope on the specimens polished with diamond up to 1 µm after mechanically polishing by emery paper up to 1200. Macro Vickers hardness values were measured with 30 kg on the 2124 specimens and 10 kg on the AS7G specimens. Micro hardness measurements have been carried out with a 20 g ($HV_{0.02}$) on the AS7G specimens. Roughness measurements on the test specimens were carried out as received and polished conditions. For the quantitative analysis, Visilog and also a medical scanner (X-rays computed tomography (CT) installed in the ITMA – CNAM/Paris, were used.

Table 1.
Nominal chemical compositions of two composites used in this study

AS7G	Si(%)	Fe(%)	Cu(%)	Mn(%)	Mg(%)	Zn(%)	Ti(%)	Other	Al
	6.5/7.5	0.15 max	0.2 max	0.1 max	0.3/0.45	0.1 max	0.2 max	0.10	balance
2124	Cu(%)	Mg(%)	Mn(%)	Si(%)	Cr(%)	Zn(%)	Fe(%)	Ti	Al
	3.84	1.33	0.46	0.05	-	-	0.09	-	balance

Tensile and fatigue tests of MMCs were conducted on an INSTRON 8501 equipped with a load cell of 10 tonnes in laboratory air at ambient temperature. Displacement rate for the tensile tests was 0.5 mm/min. All the fatigue tests were carried out at the stress ratio of 0.1 at a frequency of 30 Hz. The loading direction for all the tests is parallel to the extrusion direction. The microstructure for optical images was made by Olympus optical microscope (OM). Keller's etching was used to etch the matrix materials, which consists of 2.5 ml HNO_3, 1.5 ml HCl, 1 ml HF and 95 ml distilled H_2O. Short time etching (few seconds) was used until clear grain boundaries in the matrix. The failed specimens were examined by scanning electron microscope (SEM).

3. Results and discussion

3.1. Microstructure, roughness and hardness evaluation

Fig. 2 shows the microstructures of the sections longitudinal and perpendicular to the extrusion direction in the 2124 composite and also the microstructure of the AS7G. It is seen that SiC particles are weakly aligned in the extrusion direction. Heterogeneity is more important in the microstructure of the AS7G with a randomly distribution than that of the 2124 and the presence of the porosity in the AS7G is related to the production method.

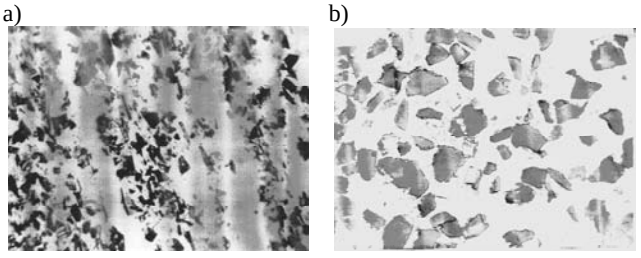

Fig. 2. Microstructures of: a) 2124 (1200X) and b) AS7G (600X) composites

The mean values (macro and micro) of Vickers hardness measurements were given in Table 2 for the as received and heat treated conditions. It can be seen that there is no difference between macro and micro hardness measurements in the as received AS7G specimens. It is noted that the increase of the hardness value after the heat treatment T6. This case is related to the aging of the matrix suitable to the treatment T6. Again, a decrease is observed after the heat treatment TS. It means that the relocation of the precipitates to the interface and the dendrites. The same evolution is observed in the micro hardness values. In other words, the hardening of the matrix appears after the T6 and a decrease in the micro hardness values after the TS. This situation can be explained that the major part of the silicon immigrated to the interface under the precipitated form after the TS.

Table 2.
Hardness measurements in two composites

AS7G	As received	Heat treated (T6)	Heat treated (TS)
Vickers Hardness (macro)	78	115	90
2124	As received		
Vickers Hardness (macro)	195		

AS7G	As received	Heat treated (T6)	Heat treated (TS)	Reinforces
Vickers Hardness (micro)	78	90	85	4250

Roughness measurements (R_a) on the specimens of two composites were taken as received and polished conditions for the evaluation of the surface effect on the fatigue behaviour. The mean values of R_a for the two composites were 0.36 μm and 0.17 μm in the case of as received and polished conditions respectively.

3.2. Tensile properties

The tensile properties of the composites studied are given in Table 3. It can be seen that the proof stress, the ultimate tensile strength and the elastic modulus increased in polished specimens. The comparison of these results explains well the important effect of the production methods, distribution of particles-homogeneity, and the size of reinforcement, etc. In any case, the 2124 showed more reliable mechanical properties than the AS7G.

Fig. 3 reveals the SEM micrographs of the fracture surfaces of the tensile specimens for each composite. For the 2124, a ductile fracture appearance was observed with shearing effects on the surface. However, the AS7G showed a typical cleavage at the surface with different facet sizes. Many microcracks and porosity were also observed.

Typical examples of crack paths on the specimen surface in the composites are shown in Fig. 4. For the 2124 composite, microcracks developed in the matrix and only a few debonding particles are observed. A high resistance interface and matrix is seen in the samples of 2124. However, crack path of AS7G is very different regarding to that of 2124. Crack developed in the matrix and in the interface. Many debonding particles with some branching of cracks are seen in the AS7G specimens.

Table 3.
Mechanical properties of the composites at ambient temperature

Composite	Proof stress $\sigma_{0.2}$ (MPa)	Ultimate tensile strength (MPa)	Elongation ε_f (%)	Reduction of area, A (%)	Elastic modulus E (GPa)
AS7G (as received)	95	247	0.47	0.15	77
AS7G (polisheed)	172	276	0.61	0.21	114
2124 (as received)	104	482	4.75	1.55	100
2124 (polished)	280	600	2	1.54	131

a) b)

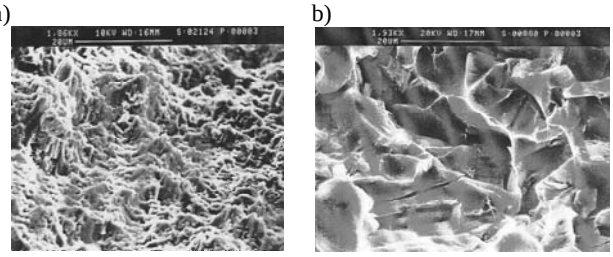

Fig. 3. Fracture surfaces of the tensile specimens for the: a) 2124 and b) AS7G composites

a) b)

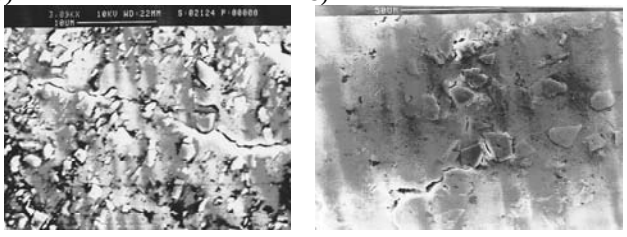

Fig. 4. Crack paths on the tensile specimens; a) 2124 and b) AS7G composites

3.3. Fatigue behaviour

Fig 5 displays the fatigue test results obtained on the two composites; 2124 and AS7G. The fatigue properties explained by S-N curves were plotted in polished and also as received conditions of the specimens for both of the two composites. These S-N curves showed that the fracture occurred between 10^6 - 10^7 cycles ranges. AS7G shows significantly lower fatigue strength with the fatigue strength at 10^6 cycles of 95 MPa regarding to 2124. The fatigue strength (σ_D) value found for 2124 is about 363 MPa [6-11]. It is seen that the particle size and the production methods are the main parameters playing an important role on the fatigue strength. These results are in agreement with the literature [1-11, 16, 19, 20, 23, 28].

a)

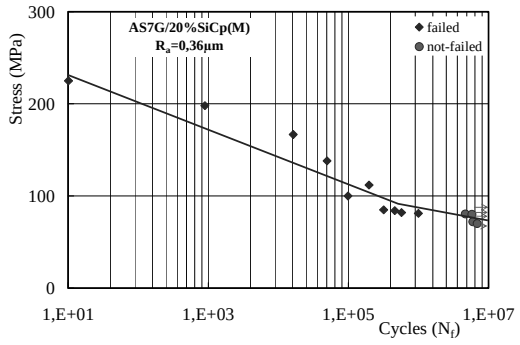

b)

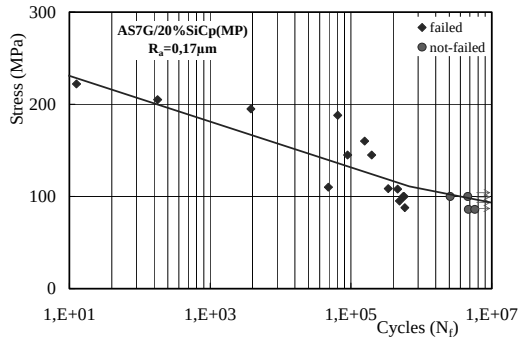

c)

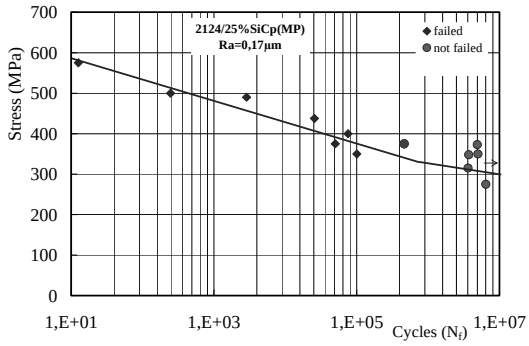

d)

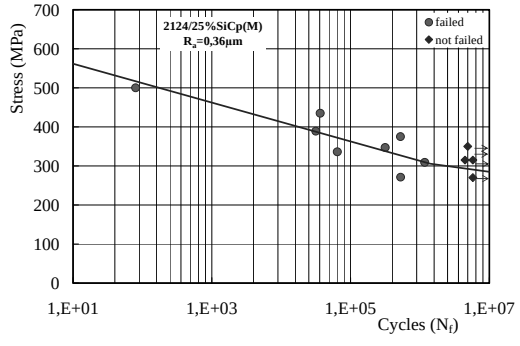

Fig. 5. Fatigue test results for two different materials at the stress ratio of 0.1 and the frequency of 30 Hz; a) AS7G (polished), b) AS7G (not polished), c) 2124 (polished), d) 2124 (not polished)

However, at high applied stresses, a considerable scatter of the data can be seen. There is no considerable effect of the surface roughness conditions on the fatigue behaviour of the composites studied here. In fact, a good correlation between fatigue strength and tensile strength are generally found in a wide variety of materials. Here, the fatigue strength decreased particularly in AS7G, thus leading to a low fatigue ratio (fatigue strength/tensile strength ratio). Such a low fatigue resistance of this composite can be attributed to a low crack initiation resistance due to the interface debonding between the SiC particles and the matrix.

Typical failure surface of the fatigue specimens of the two composites obtained by SEM were given in the Fig. 6. It can be seen that the general view of the fracture surface of 2124 is ductile with a plastic deformation area and without fatigue striations. The cracks initiated usually at defects on the specimen surface just after the first appearance of the crack. The fracture surface of the AS7G showed a facet containing the secondary cracks and the porosity. The crack generally initiated at the interface (SiC/matrix) with the interface debonding between SiC particles and the matrix, which is an essential phenomenon.

This case may be related to the particle geometry (shape) and the distribution and also the size of the particles in the matrix. These results can be compared with that of the former authors [1-4, 20-28]. Additionally, the aspect ratio of the SiC particles in the composites were found between 1.85 and 2 while the SiC particles are weakly aligned in the extrusion direction. Evidently, this situation facilitates debonding at the tip of particles and then causing to crack initiation.

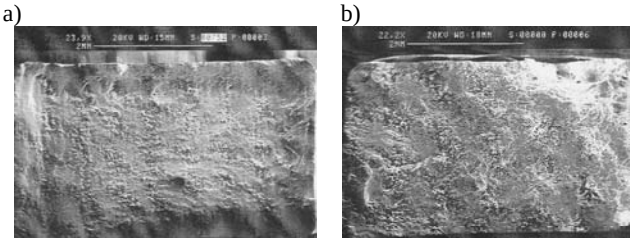

Fig. 6. Fracture surfaces of the fatigue specimens: a) 2124 and b) AS7G composites

Fig. 7 shows the crack initiation and the crack path evolution on the specimen surfaces of 2124 and AS7G composites. Firstly, the smooth crack paths are observed on the specimens of 2124. However, the crack path in the composite of AS7G is more twisted regarding to that in the 2124. More branching is observed in case of high stress levels. This case is attributed to the hard SiC particles in bigger size, which can be a barrier to the growth of small cracks and then leading to crack branching. Another cause for this case is the existence of the many short secondary cracks observed just around the principal crack on the fracture surface of the AS7G at the higher stress levels.

Additionally, a great amount of cracked particles were found just around the agglomeration of particles. However, detailed examination of the crack paths and the fracture surface of the 2124 at the higher stress ranges indicates that these cracked particles are responsible for crack initiation sites. Generally, the crack initiates from these sites and follows through the matrix. The detailed study of these specimens indicates that the interface is very weak for the higher stress ranges but strong for the lower stress ranges. Chemical analysis of the fracture surface of the 2124 showed that some particles leading to crack initiation were not the SiC particles, but they were intermetallics compounds (Al, Cu, Mn and a little amount of silicon and iron) containing very rich amount of aluminium. As a summary, much less defect and porosity were detected in the 2124.

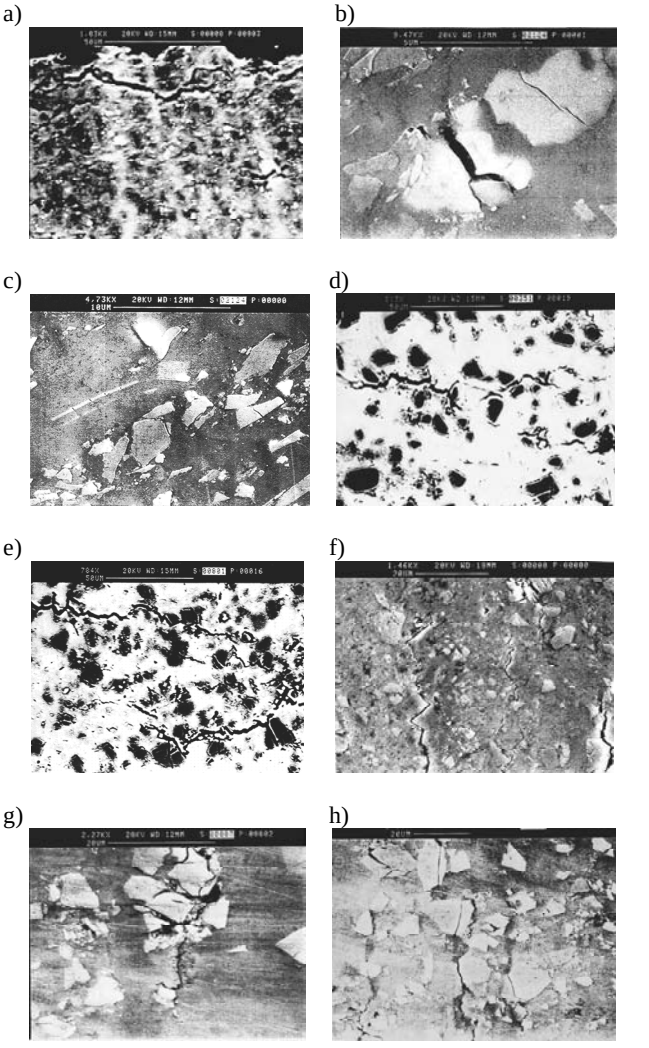

Fig. 7. Crack initiation and crack path on specimen surfaces in: a)-c) 2124 and d)-h) AS7G composites

The fractography of the fatigue specimens are in concordance with the tomography. The great interest of tomography is the possibility of viewing with a high resolution a transversal plane of an object without destroying the controlled parts. The tomography results obtained on the fatigue specimens gave very useful information about the homogeneity of the structure such as the

distribution of the reinforced particles and other defects such as an internal crack. At this stage, it is interesting to introduce a relation between the percentages of volume fractions obtained by microscopic study and the tomographic density (TD) values obtained by tomography carried on different specimens in the same direction.

Fig. 8 shows these results in order to explain a linear relation between these two different studies. Here, a parametric approach was given approximately from the variation of the volume fraction of the reinforcements as a function of the TD values.

$$V_p\ (\%) = A\ (TD - TD_o) \quad (1)$$

where TD_o is the tomographic density for the value of V_p (%) = 0.

From the experimental results obtained in this study, the parameter "A" was calculated as 0.15. So, this can be given in a simple form as follows;

$$V_p\ (\%) = 0.15\ (TD\text{-}500) \quad (2)$$

This relation can be accepted as an indicative explanation. In other words, the tomography study carried on the composites materials can characterise the particle size and the distribution of the reinforcements very well in geometrical space as 3D at the mesoscopic scale [13, 21, 26]. It is well known that the fatigue strength of MMC depends on V_p and on the repartition of particles. χ-rays tomography is shown as a possible way to study this aspect.

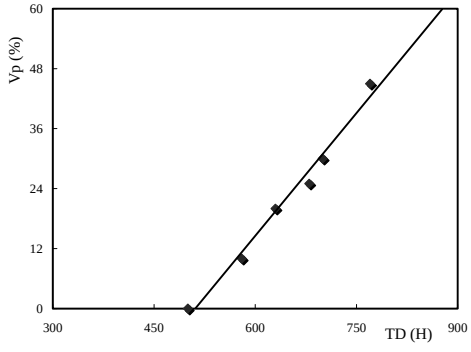

Fig. 8. Variation of volume faction depending on the tomography density (TD)

4. Conclusions

A detailed study of damage mechanism was performed using smooth specimens as received and heat treated conditions of the SiCp/2124 and AS7G composites with different production methods and different volume fraction of particles.

The AS7G composite showed considerable lower mechanical properties (tensile, fatigue strength, etc.) regarding to the 2124 composite. In the AS7G composite, the crack generally initiated at the interface (SiC/matrix) with many interface debonding between the SiC particles and the matrix. This was the principal cause of the reduced fatigue strength.

The 2124 composite showed the smooth crack paths, while the crack path in the AS7G composite were more twisted with branching in high stress levels. This is attributed to the hard SiC particles in bigger size, which can be a barrier to the growth of small cracks and then leading to crack branching. As a summary, the mechanical behaviour of these composites is related to the particle geometry (shape), the distribution and also the size of the particles in the matrix.

Applications of χ-rays CT on the composite materials is more efficient and skilful. χ-rays CT well characterise the particle size and the distribution of the reinforcements-volume fraction as 3D at the mesoscopic scale as a possible way to study this aspect.

References

[1] P.D. Pitcher, J.A. Shakesheff, J.D. Lord, Aluminium based metal matrix composites for improved elevated temperature performance, Materials Science and Technology 14 (1998) 1015-1023.

[2] T.W. Clyne, P.J. Withers, An introduction to metal matrix composites, Cambridge University Press, Cambridge, 1993.

[3] J. Lorca, Fatigue of particle-and whisker-reinforced metal-matrix composites, Progress in Materials Science 47 (2002) 283-353.

[4] T.W. Clyne, Metallic composite materials, in Physical metallurgy, Fourth Edition, Elsevier, 1996, 2568-2625.

[5] J.R. Davis, Metals handbook, Desk edition, ASM International, Materials Park, Ohio, 1998.

[6] M. Rittner, Metal matrix composites in the 21st century: markets and opportunities, CT: BCC Inc., Norwalk, 2000.

[7] D.B. Miracle, S.L. Donaldson, Introduction to composites, in ASM handbook: Composites, vol. 21, ASM International, Materials Park, Ohio, 2001, 3-17.

[8] A. Evans, C.S. Marchi, A. Mortensen, Metal matrix composites in industry: an introduction and a survey, Kluwer Academic Publishers, Dordrecht, 2003.

[9] D.L. Davidson, Fatigue and fracture toughness of aluminium alloys reinforced with SiC and alumina particles, Composites 24/3 (1993) 248-255.

[10] J.E. Spowart, D.B. Miracle, The influence of reinforcement morphology on the tensile response of 6061/SiC/25p discontinuously-reinforced aluminium, Materials Science and Engineering A 357 (2003) 111-123.

[11] D.L. Davidson, The effect of particulate SiC on fatigue crack growth in cast-extruded aluminium alloys composite, Metallurgical Transaction A 22/1 (1991) 97-112.

[12] I. Ozdemir, K. Onel, Thermal cycling behaviour of an extruded aluminium alloy/SiCp composite, Composites B 35 (2004) 379-384.

[13] E. Bayraktar, S. Antolonovich, C. Bathias, Multiscale study of fatigue behaviour of composite materials by x-ray computed tomography, Proceedings of the 3rd International Conference "Fatigue of Composites" ICFC3, Kyoto, 2004, 1322-1333.

[14] J.J. Lewandowski, C. Liu, Effects of matrix microstructure and particle distribution on fracture of an aluminium metal matrix composite, Materials Science and Engineering A 107 (1989) 241-255.

[15] Z.Z. Chen, K. Tokaji, Effect of particle size on fatigue crack initiation and small crack growth in SiC particulate-reinforced aluminium alloy composites, Materials Letters 58/17-18 (2004) 2314-2321.
[16] D.B. Miracle, Metal matrix composites - from science to technological significance, Composites Science and Technology 65 (2005) 2526-2540.
[17] S.M. Pickard, B. Derby, The deformation of particle reinforced metal matrix composites during temperature cycling, Acta Metallurgica et Materialia 38 (1990) 2537-2552.
[18] P. Cavaliere, Isothermal forging of AA2618 reinforced with 20% of alumina particles, Composites A 35 (2004) 619-629.
[19] D.B. Miracle, Metal matrix composites for space systems: current uses and future opportunities, in: Affordable metal matrix composites for high performance applications, TMS, Warrendale, 2001, 1-21.
[20] N. Chawla, C. Andres, J.W. Jones, J.E. Allison, Effect of SiC volume fraction and particle size on the fatigue resistance of a 2080 Al/SiCp composite, Metallurgical and Materials Transactions A 29 (1998) 2843-2854.
[21] A. Bouza, PhD thesis, ITMA/CNAM-Paris, 1995.
[22] D. Braz, T.R. Lopes, M.G.L. Motta, Computed tomography, Applied Radiation and Isotopes 53 (2000) 725-729.
[23] C. Fouret, S. Degallaix, Experimental and numerical study of the low-cycle fatigue behaviour of a cast metal matrix composite Al–SiCp, International Journal of Fatigue 24 (2002) 223-232.
[24] O. Hartmann, M. Kemnitzer, H. Biermann, Influence of reinforcement morphology and matrix strength of metal–matrix composites on the cyclic deformation and fatigue behaviour, International Journal of Fatigue 24 (2002) 215-221.
[25] A. Kostka, J. Lelatko, M. Gigla, H. Morawiec, A. Janas, TEM Study of the interface in ceramic-reinforced aluminium-based composites, Materials Chemistry and Physics 81 (2003) 323-325.
[26] X. Liu, PhD thesis, ITMA/Ecole Centrale-Paris, 1993.
[27] P. Poza, J. Llorca, Mechanical behaviour and failure micro mechanisms of Al/Al_2O_3 composites under cyclic deformation, Metallurgical and Materials Transactions A 26 (1995) 3131-3141.
[28] J. Llorca, P. Poza, Influence of reinforcement fracture on the cyclic stress-strain curve of metal-matrix composites, Acta Metallurgica et Materialia 43/11 (1995) 3959-3969.
[29] S.C. Tjong, NN-particles-reinforced MMCs with enhanced mechanical properties, Advanced Engineering Materials 9/8 (2007) 639-652.
[30] V. Bystritskii, E. Garate, J. Earthman, A. Kharlov, E. Lavernia, X. Peng, Fatigue properties of 2024-T3 and 7075-T6 aluminium alloys modified using plasma-enhanced ion beams, Theoretical and Applied Fracture Mechanics 32 (1999) 47-53.
[31] T.S. Srivatsan, The low-cycle fatigue behaviour of an aluminium alloy-ceramic-particle composite, International Journal of Fatigue 14 (1992) 173-182.
[32] S.B. Biner, Growth of fatigue cracks emanating from notches in SiC particulate aluminium composites, Fatigue and Fracture of Engineering Materials and Structures 13/6 (1990) 637-646.
[33] Y. Brechet, J.D. Embury, S. Tao, L. Luo, Damage initiation in metal matrix composites, Acta Metallurgica et Materialia 39 (1991) 1781-1786.
[34] J. Llorca, J.L. Martínez, M. Elices, Reinforcement fracture and tensile ductility in sphere-reinforced metal-matrix composites, Fatigue and Fracture of Engineering Materials and Structures 20/5 (1997) 689-702.
[35] M. Jain, Micromechanical stresses during low cycle fatigue of an overaged Al-Mg-Si alloy, Fatigue Fracture of Engineering Materials and Structures 15/1 (1992) 33-42.
[36] X.C. Liu, C. Bathias, Fatigue behaviour of Al_2O_3 short fibre reinforced aluminium alloy, Fatigue and Fracture of Engineering Materials and Structures 15/11 (1992) 1113-1123.